Femtosecond Mid-Infrared Study of the Reorientation of Weakly Hydrogen-Bonded Water Molecules

Sietse T. van der Post and Huib J. Bakker*

FOM Institute AMOLF, Science Park 104, 1091AG Amsterdam, The Netherlands

Supporting Information

ABSTRACT: We study the hydrogen-bond and reorientation dynamics of weakly hydrogen-bonded water molecules by studying their spectral diffusion and anisotropy dynamics with polarization-resolved two-color femtosecond mid-infrared spectroscopy. We selectively excite weakly hydrogen-bonded water molecules by tuning a relatively narrow band excitation pulse far into the high-frequency wing of the O−D stretch vibration of HDO molecules in H_2O water. We observe that the spectral diffusion and the anisotropy both show pronounced biexponential dynamics. On the basis of previous work, the fast component of the spectral dynamics with a time constant of ∼100 fs is assigned to rapid hydrogen-bond switching events. We observed that these switching events lead to a pronounced effect on the anisotropy of the excited O−D groups, which shows that the spectral relaxation is accompanied by a large change of the orientation of the O−D groups. The slow component of the spectral relaxation can be assigned to the collective structural reorganization of the hydrogen-bond network of liquid water. With increasing temperature, the spectral relaxation shows a similar acceleration as the average molecular reorientation, showing that these processes are intimately connected.

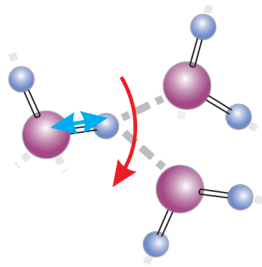

INTRODUCTION

The hydrogen-bond network of water is both robust and dynamic at the same time. The binding energy of a hydrogen bond is ∼21 kJ/mol (5.0 kcal/mol),[1,2] about one twentieth of the binding energy of the covalent O−H bond energy but still well above the energy of thermal fluctuations at room temperature. Nevertheless, in liquid water, the hydrogen bonds are quite dynamic, and water molecules rotate on a picosecond time scale. In NMR and femtosecond mid-infrared experiments, it was found that the second Legendre polynomial of the orientational correlation function of the water molecules decays with a time constant of approximately 2.5 ps.[3−8]

In femtosecond mid-infrared experiments, the time scale of molecular reorientation of the water molecules is studied by measuring the time dependence of the anisotropy of an excitation of the O−H/O−D stretch vibration. The anisotropy will decay because molecular reorientation changes the direction of the vibrational transition dipole moment. This experiment cannot be performed on pure H_2O or pure D_2O, since for these liquids the anisotropy dynamics are completely dominated by rapid coherent and incoherent energy transfer between the hydroxyl groups.[9−13] Hence, femtosecond studies of the molecular reorientation of liquid water are performed on isotopically diluted samples, i.e., on the O−H stretch vibration of HDO in D_2O or on the O−D stretch vibration of HDO in H_2O.[6−8] A study of the O−D vibration of HDO:H_2O has as an advantage that the lifetime of the O−D vibration is more than 2 times longer (∼1.8 ps) than that of the O−H vibration (∼0.75 ps), thereby allowing the measurement of the anisotropy dynamics of the excitation of the O−D group over a significantly longer time interval.

The reorientation of liquid water has also been studied theoretically with molecular dynamics simulations.[14−17] Laage and Hynes showed that the reorientation of water proceeds through a jumping mechanism in which the O−H group of a water molecule jumps over a relatively large angle of ∼60°.[14] The transition state of this orientational jump is formed by a configuration in which the reorienting hydroxyl group forms a weak bifurcated hydrogen bond with its original partner water molecule and with a new water molecule. The transition through the bifurcated state occurs on a time scale of 100 fs.[14] The presence of this energetically relatively favorable transition state (compared to a complete breaking of the hydrogen bond) explains why the molecular reorientation of water has a relatively low activation energy of 16−17 kJ/mol (3.6−4.0 kcal/mol).[17−20]

The frequencies of the hydroxyl stretch vibrations of water strongly depend on the strength of the local hydrogen bond. A strong hydrogen bond leads to a red-shift of the resonance frequency of the O−H stretch vibration, whereas a weak hydrogen bond leads to a blue-shift. Therefore, the evolution from a strong linear hydrogen bond to the weak, bifurcated hydrogen bond of the transition state for molecular reorientation is accompanied by a large change in vibrational frequency. Recently, this relation has been employed to study the mechanism of reorientation of liquid water with ultrafast 2D-IR experiments.[21] In this study, evidence for the concerted hydrogen bond switching mechanism was obtained, but the

Special Issue: James L. Skinner Festschrift

Received: February 4, 2014
Revised: April 16, 2014
Published: April 16, 2014

observed average angles are relatively small (10−20°) compared to the large angle reorientations predicted by the molecular dynamics simulations.[14] This difference could be due to the fact that the experimental data contain contributions from water molecules that undergo translational motions or only small-angle fluctuations, i.e., that are not involved in a successful switching of their hydrogen bond.

Here we study the mechanism of reorientation of liquid water with two-color femtosecond mid-infrared spectroscopy. We use relatively narrow-band excitation pulses tuned to the far blue wing of the absorption band of the O−D stretch vibration of HDO in H_2O. Thereby, we selectively excite very weakly hydrogen-bonded HDO molecules that will have a high probability of being close to the transition state for molecular reorientation. The excitation of weakly hydrogen-bonded molecules was included in a previous study of our group of the anisotropy dynamics of liquid water at room temperature.[22] Here we use a more selective excitation of these molecules by using a more narrow excitation spectrum, and we use a new improved method to correct for thermal effects, which is essential to obtain accurate anisotropy dynamics in this region of the absorption band. We combine the anisotropy dynamics with measurements of the spectral relaxation, and we determine the temperature dependence of these relaxation processes in the temperature range from 283 to 343 K. Thereby, we obtain information on the intimate relation between the collective structural reorganization of the hydrogen-bond network and the molecular reorientation of water.

EXPERIMENT

The mid-infrared pump pulses of the polarization-resolved two-color pump−probe experiment were generated by two subsequent optical parametric amplification (OPA) processes. The first process was performed in a commercial OPA (LightConversion TOPAS) and was pumped by 800 nm pulses with an energy of 850 μJ per pulse. The 800 nm pulses are a fraction of the output of a regenerative Ti:sapphire laser (Coherent), providing pulses with a duration of 35 fs and a total pulse energy of 3.5 mJ at a repetition rate of 1 kHz. In the OPA, the 800 nm pulse is converted to a signal pulse and an idler pulse with a wavelength of ∼2 μm. The idler pulse is frequency doubled to ∼1 μm using a relatively long β-barium-borate (BBO) crystal of 4 mm. This crystal has a small acceptance bandwidth leading to a narrow-band seeding pulse for the second parametric amplification stage. In this second parametric amplification stage, a relatively long (10 mm) lithium niobate crystal was used to generate narrow-band mid-infrared pulses around 4 μm. The thus obtained mid-infrared pulses had a pulse energy of 16 μJ and a spectral bandwidth of ∼60 cm^{-1}. The center frequency was tuned to the blue wing of the absorption band (2650 cm^{-1}) to selectively excite O−D groups that donate a very weak hydrogen bond. The cross correlate of the narrow band pump pulses and the probe pulses at 2650 cm^{-1} measured in a thin germanium window was 250 fs.

The probe pulses are generated with a home-built OPA that is pumped with 800 nm pulses with an energy of 850 μJ. The home-built OPA is white-light seeded and generates signal and idler pulses in a BBO crystal (2 mm). The signal and idler pulses are difference frequency mixed in a silver-gallium-disulfide crystal (1.2 mm), yielding mid-IR pulses of which the center frequency was tuned to 2200, 2550, or 2950 cm^{-1}. The full width at half-maximum (fwhm) of the pulse spectra was 300 cm^{-1}.

We excited the O−D stretch vibration of HDO molecules in isotopically diluted water with the intense mid-infrared laser pulse. The excitation modifies the absorption spectrum: at the fundamental transition frequencies of the O−D stretch vibration, the absorption is decreased (bleached) due to the partially depleted ground state and $\nu = 1 \rightarrow 0$ stimulated emission. In addition, the excitation of $\nu = 1$ leads to a new absorption at the $\nu = 1 \rightarrow 2$ transition frequency. The absorption changes $\Delta\alpha$ vanish on a picosecond time scale due to vibrational relaxation. The dynamics of $\Delta\alpha(\nu, t)$ are monitored by measuring the transmission of the weak probe pulse for varying pump−probe delay times t. After the vibrations have decayed, the absorbed pump energy thermalizes into low frequency bath modes. As a result of the thermalization, the sample temperature increases with 5 K in the focus of the pump beam.

The pump pulse is linearly polarized and creates a directional anisotropy of the excited subset of O−D oscillators. This anisotropy decays as a result of molecular reorientation. These dynamics are determined by performing measurements with probe pulses that are polarized parallel and perpendicular to the polarization of the pump pulse. The dynamics of the thus measured absorption changes $\Delta\alpha_{\parallel}(\nu, t)$ and $\Delta\alpha_{\perp}(\nu, t)$ represent vibrational relaxation, spectral diffusion, and molecular reorientation. From $\Delta\alpha_{\parallel}(\nu, t)$ and $\Delta\alpha_{\perp}(\nu, t)$, we can construct the isotropic absorption changes $\Delta\alpha_{iso}(\nu, t)$ that represent the vibrational relaxation and spectral diffusion only:

$$\Delta\alpha_{iso}(\nu, t) = \frac{\Delta\alpha_{\parallel}(\nu, t) + 2\Delta\alpha_{\perp}(\nu, t)}{3} \quad (1)$$

From $\Delta\alpha_{\parallel}(\nu, t)$ and $\Delta\alpha_{\perp}(\nu, t)$, we can also construct the anisotropy parameter $R(\nu, t)$:

$$R(\nu, t) = \frac{\Delta\alpha_{\parallel}(\nu, t) - \Delta\alpha_{\perp}(\nu, t)}{\Delta\alpha_{\parallel}(\nu, t) + 2\Delta\alpha_{\perp}(\nu, t)} \quad (2)$$

In the absence of spectral diffusion (or after the spectral diffusion is complete), $R(\nu, t)$ only represents the dynamics of the molecular reorientation, as the dynamics due to vibrational relaxation are divided out.

SAMPLES

We used D_2O (99.9% pure, Sigma-Aldrich) and Millipore water to make isotopically diluted water samples (8 mol % D_2O in H_2O). We used this isotope ratio to obtain an optimal contrast between the signal from the O−D stretch vibration and the signal coming from the thermalization of excited O−H stretch vibrations, while keeping resonant Förster energy transfer at a minimum.[11] The sample cell consisted of a stainless steel ring with two calcium fluoride windows (0.5 mm), pressed against each other with a 25 μm spacer in between. The temperature of the sample cell is varied with a Peltier cooling element and with a heating element that heats the aluminum base plate of the sample cell. A thermocouple attached to the sample cell and a feed-back loop were used to maintain a constant temperature ($\Delta T \approx \pm 1$ K) in the temperature range 283−343 K.

RESULTS AND DISCUSSION

Isotropic Spectra. We construct isotropic transient spectra from the measured $\Delta\alpha_{\parallel}(\nu, t)$ and $\Delta\alpha_{\perp}(\nu, t)$ using eq 1. In Figure 1, we show transient spectra at different delay times

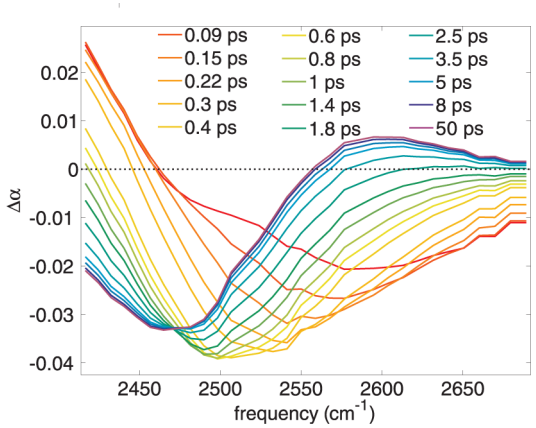

Figure 1. Isotropic transient spectra for pump−probe delay times between 0.09 ps (red line) and 50 ps (purple line). The excitation pulse is centered at 2650 cm^{-1} and has a bandwidth of ~60 cm^{-1}. At short delay times, the transient spectra mainly show a bleach at frequencies >2450 cm^{-1}. The bleach subsequently shifts to lower frequencies and decays. At long delay times, the transient spectrum takes the form of a thermal difference spectrum.

following excitation with a narrow-band pump pulse centered at 2650 cm^{-1}. For short delay times, the transient spectra show a bleach in the blue wing of the absorption band due to the depletion of the vibrational $v = 0$ ground state, leading to a decrease in $v = 0 \rightarrow 1$ absorption and stimulated $1 \rightarrow 0$ emission out of the excited $v = 1$ vibrational state. With increasing delay times, the bleaching signal shifts to lower frequencies and decays. The frequency shift indicates the presence of fast spectral diffusion of the excited O−D oscillators. After 30 ps, the spectrum is not changing anymore with increasing delay time within the experimentally accessible range (1 ns). This quasi-static transient spectrum is the thermal difference spectrum that arises from the increase of the sample temperature following vibrational relaxation.

Thermalization Dynamics. To determine the spectral diffusion and reorientation dynamics of only the excited O−D oscillators, the absorption changes $\Delta\alpha_{\parallel}(\nu, t)$ and $\Delta\alpha_{\perp}(\nu, t)$ should only represent the transient absorption signal associated with the excitation of these oscillators. Hence, $\Delta\alpha_{\parallel}(\nu, t)$ and $\Delta\alpha_{\perp}(\nu, t)$ should be corrected for the contribution of thermal effects to the transient spectrum. In previous work, this correction was performed by fitting a kinetic relaxation model to the isotropic data in order to obtain the shape and dynamics of the thermal difference spectrum.[22,23] This approach works reasonably well if the O−D stretch absorption band is excited near its center (2500 cm^{-1}), as in that case only O−D oscillators are excited that show a nearly frequency-independent relaxation time of 1.8 ps. However, when the excitation pulse is tuned to the wings of the O−D stretch absorption spectrum, not only O−D oscillators will be excited but also modes of the background H_2O solvent. Although 2650 cm^{-1} is far from the maximum of 3400 cm^{-1} of the O−H stretch absorption band of H_2O, the absorption of O−H oscillators is non-negligible, because H_2O is the main constituent of the sample, and because the O−H stretch absorption band is extremely broad as a result of strong intra- and intermolecular couplings.[24] The vibrational relaxation of the O−H stretch vibrations of H_2O has a time constant of ≈200 fs,[25] and is thus much faster than the vibrational relaxation of the O−D vibration of HDO. As a result, the thermal contribution to the transient spectrum will show an additional rapid rising component. In view of this complication, we determine the thermalization dynamics with a different method.

Figure 2A shows that, upon heating a sample containing 8% HDO:H_2O by a few degrees, virtually all modes in the linear spectrum of water from 400 to 4000 cm^{-1} either shift or change in amplitude. We are thus able to measure the dynamics of the thermal difference spectrum by probing a part of the spectrum where there is very little contribution from the excitation itself. We chose to probe the large thermal response in the red wing of the O−H stretch vibrations of H_2O, around 3000 cm^{-1}.

Figure 2B shows the results of a measurement in which the O−D stretch vibration is excited with a narrow-band excitation pulse at 2650 cm^{-1} and a detection pulse centered at 2950 cm^{-1}. At short delay times, the transient spectrum shows an induced absorption at low frequencies. This feature quickly decays, after which a bleach at higher frequencies grows in at a much slower rate. We recognize the shape of the bleach as the

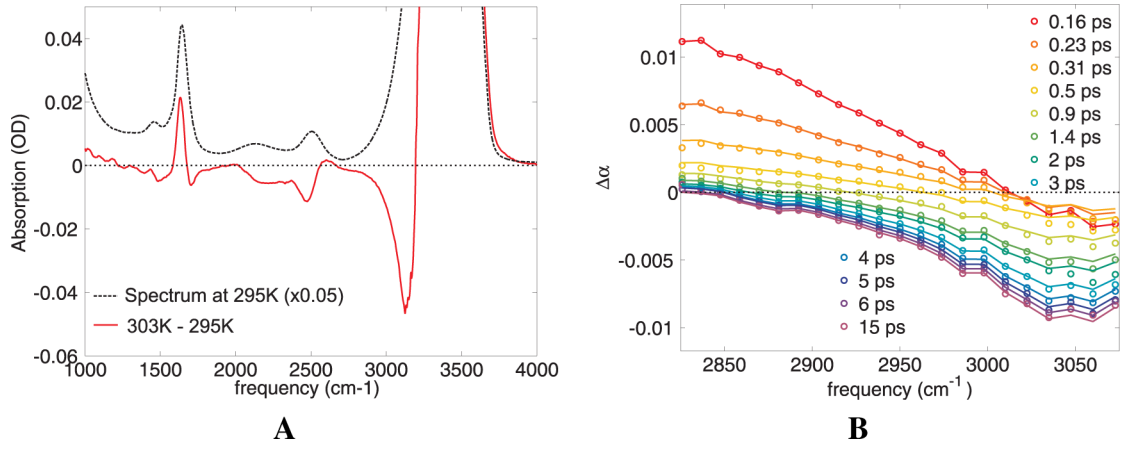

Figure 2. (A) Linear spectrum of a sample of 8% HDO in H_2O at 295 K (multiplied by 0.05, dashed line) and the difference spectrum between a linear spectrum at 295 K and a linear spectrum of the same sample at 303 K. The difference spectrum shows many features, caused by the shifting of bands and changes in cross sections upon a rise in temperature. (B) Transient spectra for different delay times probed around 2950 cm^{-1} after exciting the O−D stretch vibration in a sample of 8% HDO:H_2O with a pump centered at 2650 cm^{-1}. The bleach that rises with increasing delay time is the thermal difference spectrum of the red wing of the O−H stretch vibrations of H_2O.

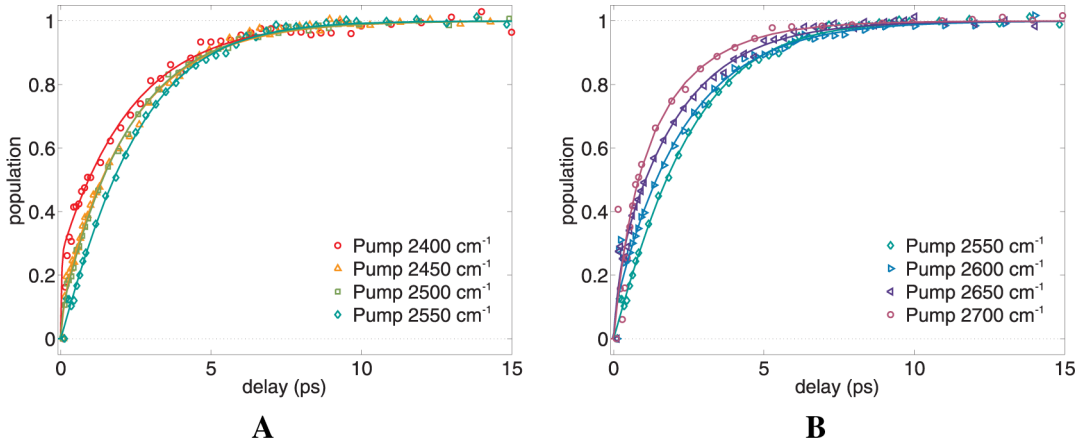

Figure 3. Thermalization dynamics measured for different center frequencies of the pump red-shifted (A) and blue-shifted (B) from the center of the O−D stretch absorption band. The initial dynamics becomes faster with increasing red-shift or blue-shift with respect to the center of the O−D stretch absorption band.

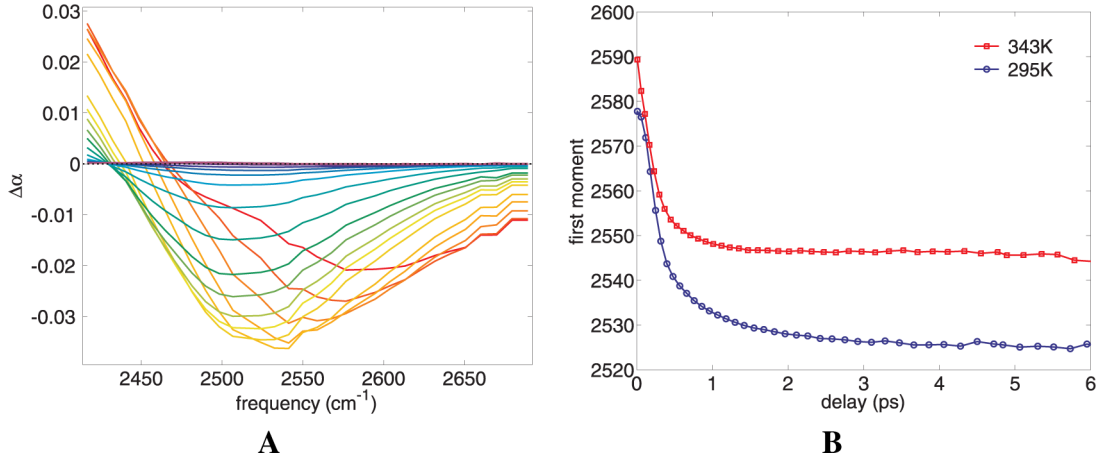

Figure 4. (A) Isotropic transient spectra from which the thermalization component is subtracted. The first moment M_1 of the bleaching part of the transient spectra is plotted in panel B for sample temperatures of 295 and 343 K. The time evolution of the first moment M_1 reflects the spectral diffusion of the excited O−D stretch vibrations.

thermal difference spectrum in this spectral region (see Figure 2A). The spectral response at short delay times arises from the $v = 1 \rightarrow 2$ transition of O−H oscillators that are excited in the far red wing of the O−H stretch absorption band. The O−H stretch excited state spectrum and the thermal difference spectrum show quite different shapes and dynamics. Hence, the transient spectra measured near 2950 cm^{-1} can be easily decomposed in these two spectral contributions. In this decomposition, we take the transient spectra at long delay times (100 ps) as the spectral shape of the thermal difference spectrum, because at these delay times the O−H stretch vibrations have completely relaxed. For the spectral shape of the O−H stretch excited state spectrum, we use the transient spectrum at 150 fs. At this delay time, the pump and probe pulse are not overlapping anymore and the contribution of a possible coherent artifact will be negligible.

Figure 3 shows the dynamics of the thermal difference spectrum resulting from a decomposition of the transient spectra in the frequency region around 2950 cm^{-1} for different central frequencies of the excitation pulse. The dynamics clearly depend on the excitation spectrum, and show a faster initial rise in case the O−D stretch absorption band is not pumped in the center at 2500 cm^{-1}. If the pump spectrum is shifted to frequencies higher than 2550 cm^{-1} (Figure 3A), this initial rise is due to the excitation of O−H stretch vibrations. For excitation frequencies in the red wing of the O−H stretch absorption band (Figure 3A), a similar fast initial rise results from the excitation of the blue wing of the H_2O-bend plus libration band at 2200 cm^{-1}. In ref 20, it was observed that the thermal effects resulting from the excitation of the background H_2O solvent lead to a distortion of the 2D-IR spectrum, especially at later delay times. At elevated temperatures, the background thermal effects were observed to lead to a residual offset for the slope of the phase lines of the 2D spectrum. The distortion of the 2D spectrum can be explained from the fact that the relative amount of background H_2O absorption becomes larger with increasing detuning of the excitation frequency from the center of the O−D stretch absorption band. Hence, the background thermal effect has a much larger effect on the transient spectrum for an excitation in the blue wing than in the center of the absorption band.

To obtain accurate spectral relaxation and anisotropy dynamics, we correct the measured $\Delta\alpha_{\parallel}(\nu, t)$ and $\Delta\alpha_{\perp}(\nu, t)$ at each delay time for the contribution arising from the excitation of the background H_2O solvent. For each experiment of the O−D stretch vibration, we determine the dynamics of

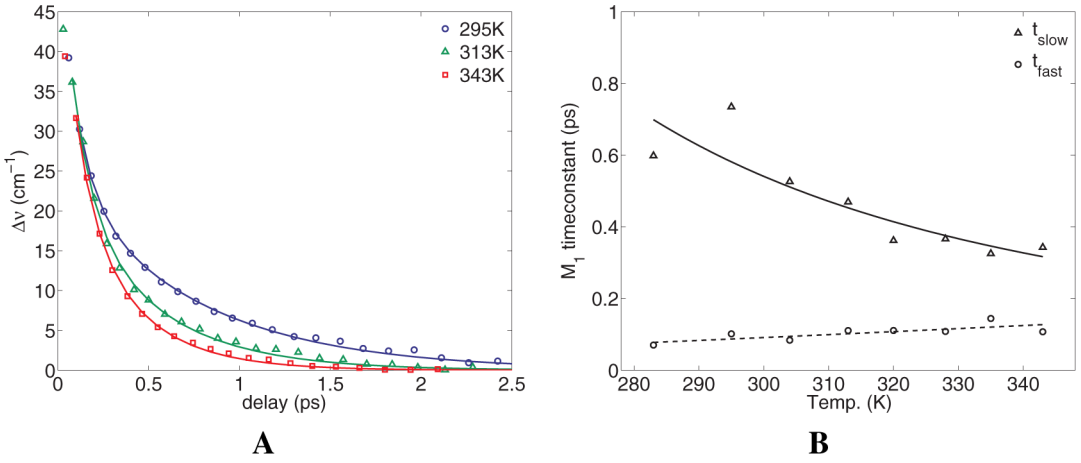

Figure 5. (A) The first spectral moment M_1 of the bleaching part of the transient spectrum as a function of delay time for three different temperatures. The first moments M_1 are given as the frequency difference with respect to its final value, to facilitate the comparison of the dynamics at different temperatures. The solid lines represent a fit to the original data of a biexponential function plus an offset (equilibrium frequency). For a better comparison of the dynamics at various temperatures, the equilibrium frequency was subtracted from both the data and the fits. (B) Time constants of the fast and slow components of the dynamics of M_1 as a function of temperature.

the thermalization with a separate experiment in which we measure the response in the frequency range around 2950 cm^{-1} induced by the same excitation pulse. We fit the rise of the thermal difference spectrum in this frequency range with a multiexponential function. Typically, a function of three exponentials is found to accurately describe the curves (solid lines in Figure 3). We use these dynamics to correct the measured $\Delta\alpha_{\parallel}(\nu, t)$ and $\Delta\alpha_{\perp}(\nu, t)$ at all delay times for the contribution of the thermal difference spectrum in the frequency region of the O−D stretch vibration. The spectral shape of the thermal difference spectrum in this frequency region is determined by averaging the measured transient spectra between delay times of 70 and 100 ps (when the O−D stretch vibration has completely relaxed).

Spectral Diffusion. In Figure 4A, we present the isotropic data obtained after subtraction of the delay-dependent thermal difference spectrum following the procedure of the previous subsection. The maximum of the bleaching signal shows a strong red-shift with increasing delay time, showing the presence of spectral diffusion effects. To quantify the spectral diffusion, we evaluate the first moment M_1 of the negative (bleaching) part of the heat-corrected transient spectra. In Figure 4B, the first moment is plotted as a function of the pump probe delay time. The value of M_1 starts at 2610 cm^{-1}, in between the maximum of the excitation spectrum at 2650 cm^{-1} and the maximum of the absorption spectrum at 2520 cm^{-1}. If the absorption band would have been completely homogeneously broadened, M_1 would have started at the maximum of the absorption band at 2520 cm^{-1} and thus would have shown no dynamics. The starting value of M_1 differs from 2520 cm^{-1} because the absorption band is inhomogeneously broadened. The absorption band can be viewed as a distribution of more narrow homogeneous line shapes, of which the number density falls off in the wings. Hence, an excitation pulse at 2650 cm^{-1} has a higher excitation probability for homogeneous line shapes of O−D oscillators that are red-shifted from 2650 cm^{-1} than for O−D oscillators that are resonant at 2650 cm^{-1}. As a result, the initial value of M_1 is at 2610 cm^{-1}. We observe that M_1 shows a rapid partial decay. Within a few hundred femtoseconds, M_1 has already relaxed to ~2560 cm^{-1}. The decay of M_1 continues in the subsequent 1.5 ps, reaching a final frequency value of 2530 cm^{-1}. This frequency is somewhat higher than the maximum of the linear absorption spectrum of the O−D stretch vibration because the transition spectrum also contains the excited state $v = 1 \rightarrow 2$ absorption that competes with the bleaching of the fundamental $v = 0 \rightarrow 1$ transition. At 343 K, the final frequency of M_1 is higher and the decay is faster than at 295 K. The higher final frequency results from the blue-shift of the linear absorption spectrum of the O−D stretch vibration with temperature.

In Figure 5A, we present the first moment as a function of delay time measured at three different temperatures. It is seen that the decay of the first moment becomes faster as the temperature increases. At all temperatures, a biexponential function plus offset was fitted to the measured M_1 dynamics (the offset was subtracted for clarity in Figure 5A). The fitted time constants of the fast and slow components are presented for all data in Figure 5B and in Table 1. The time constant of the fast component shows very little dependence on temperature, whereas the time constant of the slow component decreases with increasing temperature.

Anisotropy Dynamics. The thermally corrected $\Delta\alpha_{\parallel}(\nu, t)$ and $\Delta\alpha_{\perp}(\nu, t)$ are used to determine the dynamics of the anisotropy $R(\nu, t)$ using eq 2. In Figure 6A, the anisotropy is shown as a function of delay time for five different detection

Table 1. Fitted Time Constants of Bi-Exponential Fits to the Decay of the First Moment ($t_{M_1,1}$, $t_{M_1,2}$) and to the Anisotropy Decay at 2600 cm^{-1} ($t_{R,1}$, $t_{R,2}$) at Different Temperatures[a]

T (K)	$t_{M_1,1}$	$t_{M_1,2}$	$t_{R,1}$	$t_{R,2}$
283	0.07	0.60	0.41	3.21
295	0.10	0.73	0.41	2.48
304	0.08	0.53	0.39	2.38
313	0.11	0.47	0.28	1.75
320	0.11	0.37	0.32	1.49
328	0.11	0.37	0.29	1.53
335	0.14	0.33	0.28	1.39
343	0.11	0.34	0.30	1.24

[a]All time constants are in picoseconds.

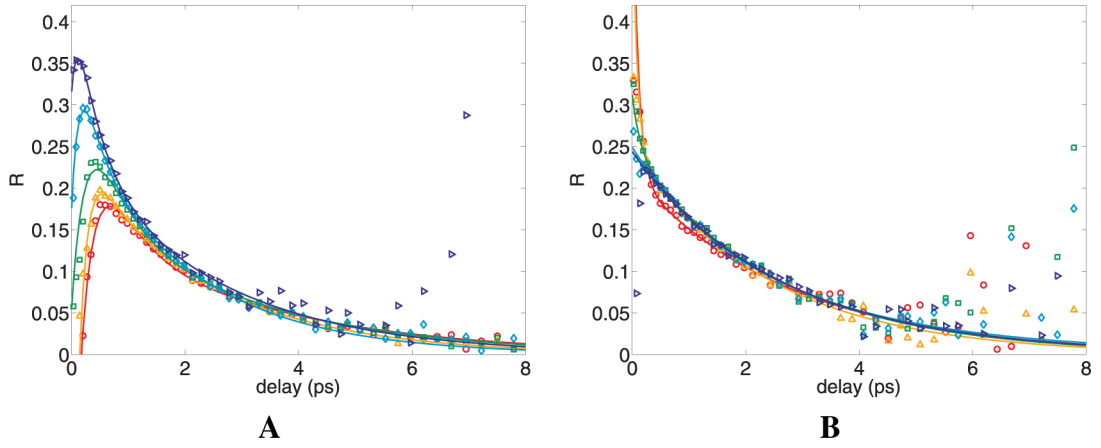

Figure 6. Anisotropy dynamics of the O−D stretch vibration of HDO in H_2O. The O−D stretch vibration is excited with a narrow-band excitation pulse centered at 2650 cm^{-1}. (A) Anisotropy at detection frequencies in the $\nu = 0 \rightarrow 1$ region (2490, 2500, 2520, 2560, and 2600 cm^{-1}, red to blue curves). For short delay times, the anisotropy has a strong dependence on the detection frequency. (B) Anisotropy at detection frequencies in the $\nu = 1 \rightarrow 2$ region (2100, 2150, 2200, 2250, and 2300 cm^{-1}, red to blue curves). The anisotropy dynamics show little frequency dependence and decay with a time constant of 2.3 ± 0.2 ps.

frequencies. It is seen that the anisotropy dynamics strongly differ for different detection frequencies in the first picosecond after the excitation, while for longer delay times the anisotropy becomes frequency independent. For low probe frequencies (for example, at 2500 cm^{-1}), the anisotropy has a low initial value and rises to a maximum value. After ∼1.5 ps, the anisotropy has the same value at all frequencies and shows the same exponential decay with a time constant of ∼2.5 ps. This time constant is identical to the time constant of water reorientation after a broad excitation pulse.[8]

Figure 6A shows that the anisotropy acquires very low (even negative) initial values at frequencies <2500 cm^{1}. This observation can be explained from the fact that the total transient spectrum is a combination of a (negative) bleaching signal at the $\nu = 0 \rightarrow 1$ transition frequencies and a (positive) induced absorption signal at the $\nu = 1 \rightarrow 2$ transition frequencies. The induced absorption is red-shifted about 180 cm^{-1} with respect to the bleach. Therefore, a considerable spectral region exists in which both features overlap. As a result, the total measured transient absorption at 2500 cm^{-1} represents the bleaching of the fundamental absorption at this frequency and the blue wing of the induced $\nu = 1 \rightarrow 2$ absorption of O−D oscillators for which the fundamental $\nu = 0 \rightarrow 1$ transition frequency is much higher, i.e., at ∼2650 cm^{-1}. If the anisotropy does not depend on frequency, the addition of the bleaching and induced absorption of different oscillators will not affect the net value of the anisotropy. However, if there is a frequency dependence of the anisotropy, this dependence will be amplified, which can be explained as follows. If the anisotropy decreases with increasing O−D frequency, the anisotropy of the bleaching at 2500 cm^{-1} will be larger than that of the induced absorption at 2500 cm^{-1}, as this latter absorption represents the high-frequency wing of the $\nu = 1 \rightarrow 2$ transition. This means that a relatively small induced absorption $\Delta\alpha_{\parallel}(\nu, t)$ is subtracted from the bleaching $\Delta\alpha_{\parallel}(\nu, t)$ and a relatively large induced absorption $\Delta\alpha_{\perp}(\nu, t)$ is subtracted from the bleaching $\Delta\alpha_{\perp}(\nu, t)$. Hence, subtraction of an induced absorption with a low anisotropy will increase the ratio of $\Delta\alpha_{\parallel}(\nu, t)$ and $\Delta\alpha_{\perp}(\nu, t)$ of the residual bleaching signal, thus amplifying the increase of the anisotropy with decreasing O−D frequency. Vice versa, if the anisotropy decreases with decreasing frequency, an induced absorption with a relatively large anisotropy is subtracted from a bleaching signal with a relatively low anisotropy, thus making the anisotropy of the residual even lower and potentially even negative (meaning that the residual $\Delta\alpha_{\perp}(\nu, t)$ > residual $\Delta\alpha_{\parallel}(\nu, t)$). This situation applies to the results shown in Figure 6A (see also the Supporting Information).

The complicating effects on the anisotropy of the competition between the $\nu = 0 \rightarrow 1$ bleaching and the $\nu = 1 \rightarrow 2$ induced absorption can be avoided by probing the red wing of the induced absorption only. In Figure 6B, the anisotropy dynamics measured between 2100 and 2300 cm^{-1} are shown, using the same spectrally narrow excitation pulse centered around 2650 cm^{-1}. It is seen that the anisotropy remains positive at all frequencies and in fact shows very little frequency dependence, thanks to the fact that there is no interference with the $\nu = 0 \rightarrow 1$ bleaching signal. The initial value of ∼0.2 is quite low which shows that the excitation in the blue wing leads to a relatively low value of the anisotropy in the red wing of the O−D absorption band.

Figure 7 shows the frequency-dependent dynamics of the anisotropy measured at T = 328 K. The vibrational lifetime T_1 of the O−D stretch vibration becomes longer for increasing temperature,[17,26] which makes it easier to determine the anisotropy at long delay times. Comparison with the data

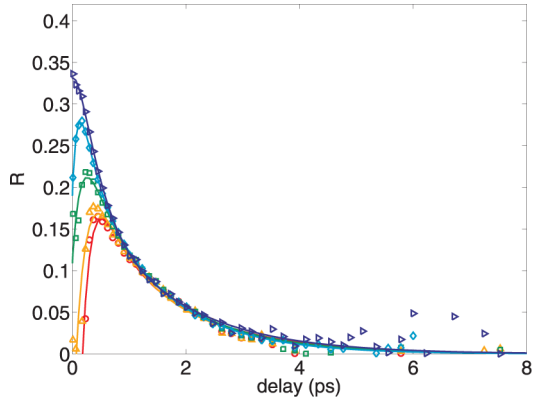

Figure 7. Similar figure as Figure 6A (identical probe frequencies) for a sample temperature of 328 K.

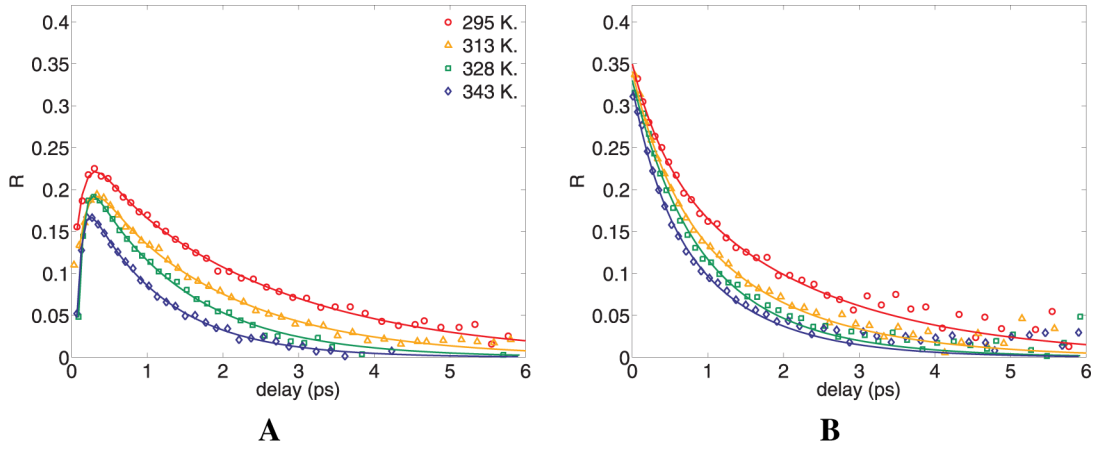

Figure 8. Anisotropy decay probed at 2500 cm^{-1} (A) and at 2600 cm^{-1} (B) after excitation by a spectrally narrow pump centered at 2650 cm^{-1}, for sample temperatures of 295 K (circles), 313 K (triangles), 328 K (squares), and 343 K (diamonds).

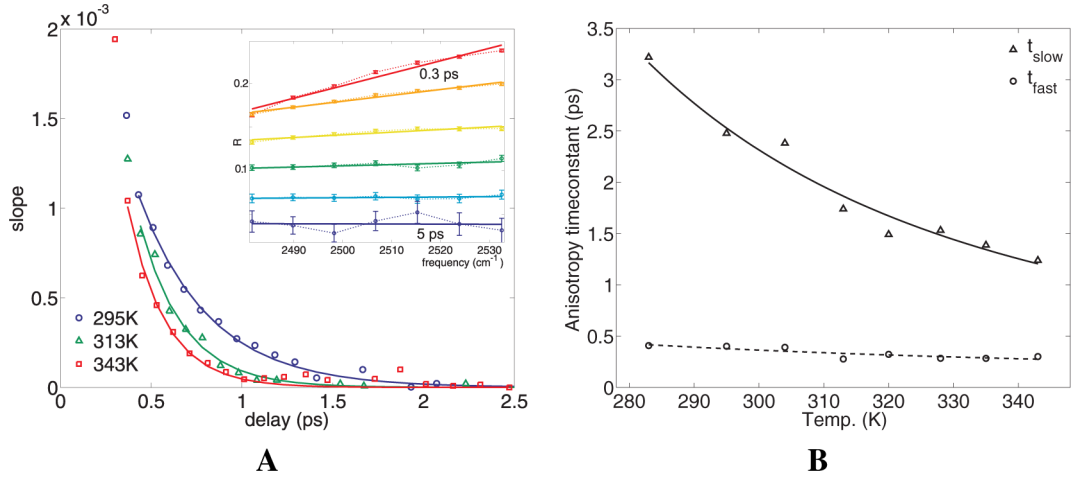

Figure 9. (A) The slope of a straight line fitted to the anisotropy as a function of frequency between 2485 and 2530 cm^{-1}, as a function of delay time for a number of temperatures. The solid lines represent exponential fits to the data. The inset shows the fitted slopes (solid lines) at different delay times for the frequency-dependent anisotropy data at 295 K. (B) The time constant of the anisotropy slope dynamics of panel A and the time constant of the long-time (average) anisotropy decay as a function of temperature.

presented in Figure 6 shows that the anisotropy relaxes significantly faster at 328 K than at 295 K. In Figure 8, the anisotropy decays at 2500 cm^{-1} (left panel) and 2600 cm^{-1} (right panel) are shown for four different sample temperatures. It is clearly seen that the anisotropy decay speeds up with increasing temperature. This speed up is in line with previous work in which it was shown that the average reorientation of water closely follows the Stokes−Einstein−Debye relation.[18,26]

We quantify the equilibration dynamics of the anisotropy in the first picosecond by fitting a straight line to the frequency-dependent anisotropy at every delay time. The slope represents the frequency dependence of the anisotropy. Figure 6a shows that the anisotropy depends on the probe frequency at short delay times. The inset of Figure 9A shows the value of the anisotropy parameter as a function of probe frequency for various delay times. We fitted a straight line to the curves in the inset to quantify the frequency dependence: a slope of zero would mean no frequency dependence. The nonzero slope at short delay times decays with increasing delay time, which shows that an equilibration takes place: initially, the reorientation depends on the probe frequency, but after a certain time, it does not anymore. This equilibration of the anisotropy is due to the spectral diffusion. In Figure 9B, we show the slope values as a function of pump−probe delay time for a number of temperatures. We fitted the slope decays to an exponential function (solid lines), thus obtaining spectral equilibration time constants at different temperatures. The resulting time constants are shown in Figure 9B for all temperatures and obey Arrhenius behavior (dashed line). In addition, we present the time constants of the frequency-independent anisotropy decay observed for delay times >1.5 ps, also following Arrhenius behavior (solid line). The time constants are given in Table 1.

Interpretation and Discussion. *Inertial Spectral and Orientational Relaxation.* The relaxation of the first spectral moment M_1 shown in Figures 4 and 5 shows an initial fast component with a time constant of ∼100 fs. The presence of this fast component agrees with the results of Loparo et al.[27] In this work, a large amplitude fast component in the spectral diffusion was observed in the case of excitation in the blue wing of the O−H stretch vibration of HDO molecules in D_2O. In view of the high excitation frequency, the fast component is associated with water molecules for which the hydroxyl group is at a large distance from its hydrogen-bonded partner (large R_{O-O} distance) and/or for which the angle between the O−H coordinate and the O−O coordinate has a large value.

Molecular dynamics simulations showed that the strained hydrogen-bond configuration can be more or less symmetric, in case the O−D group donates two weak hydrogen bonds to two water molecules at similarly large R_{O-O} distances and with similarly large angles between the R_{O-O} coordinate and the excited O−D coordinate.[14,27] Such a configuration can evolve to a fully symmetric bifurcated transition state for switching of the hydrogen-bonded partner. This transition state can rapidly fall back (unsuccessful jump) to a single strong hydrogen bond with the original hydrogen-bonded partner or rapidly evolve to a new strong hydrogen bond with the new partner (successful jump).[14] Irrespective of whether the hydrogen bond is symmetrically or asymmetrically strained, the strained hydrogen-bond configuration will quickly relax to a single strong hydrogen bond, thus leading to a strong decrease of the excited O−D vibrational frequency.

The relaxation of the strained hydrogen-bond configurations is accompanied by a large change of the orientation of the excited O−D group. Hence, this relaxation will lead to a decay of the anisotropy. The relaxation of the strained hydrogen-bond configurations will thus give rise to a low-anisotropy signal with a spectral dependence given by the linear absorption spectrum. In the case of narrow-band excitation in the blue wing, there will be very few HDO molecules directly excited in the center and the red wing of the absorption band. Hence, at early delays, the signal observed in the center and the red wing will be dominated by the low-anisotropy signal of relaxed O−D groups that were originally excited in a strained hydrogen-bond configuration. Indeed, the anisotropy in the center and the red wing is observed to be low directly after the excitation, as seen in Figures 6A and 7A.

There can also be inertial reorientation motions that do not lead to a significant change of the frequency. For instance, the inertial motion can bring the strained hydrogen-bond configuration to a new but similarly strained hydrogen-bond configuration, thus retaining the high hydroxyl stretch frequency. If the O−O distance is large, then there can also be orientational fluctuations around this hydrogen bond that hardly change the frequency (the hydrogen bond remains weak for all orientations of the hydroxyl group). These orientational fluctuations are often denoted as librational (hindered rotational) motions and can also occur for stronger (shorter) hydrogen bonds, albeit with a smaller angular cone.[7,15,28,29] At room temperature, the contribution of librations to the decay of the anisotropy of the O−D stretch vibration of HDO:H_2O ranges from ∼7% at the maximum of the absorption band to ∼15% in the blue wing of the absorption band.[15] These anisotropy decays correspond to relatively small cone angles ranging from 12 to 18°.

In the blue wing of the absorption band, the frequency-conserving inertial motions are of a relatively large amplitude, thus leading to a significant drop of the anisotropy from 0.4 to ∼0.35. Nevertheless, in the case of excitation in the blue wing, the signal at early delay times will be dominated by excited HDO molecules in strained hydrogen-bond configurations that have not yet undergone an orientational relaxation (e.g., switching) to a strong hydrogen bond and that have only experienced a partial frequency-conserving inertial reorientation. Therefore, at early delay times, the anisotropy in the blue wing will be relatively high compared to the anisotropy in the center and the red wing of the absorption band, where the signal will be dominated by excited HDO oscillators that underwent a full relaxation process from a strained hydrogen bond to a relaxed and strong hydrogen bond (Figures 6A and 7A).

The frequency dependence of the anisotropy is largely consistent with the results reported by the Tokmakoff group in a 2D-IR study of the anisotropy dynamics of the O−H stretch vibration of HDO in D_2O.[21] The absorptive 2D-IR anisotropy spectra presented in this study also show a somewhat lower anisotropy in the center of the absorption band following excitation in the blue wing of the O−H stretch vibration, in agreement with the present findings. However, the frequency dependence is less pronounced and the corresponding power spectra did not show this frequency dependence of the anisotropy. This difference cannot be due to the interference of the $v = 0 \rightarrow 1$ bleaching signal and the $v = 1 \rightarrow 2$ induced absorption, as this interference will only amplify the frequency dependence of the anisotropy. Hence, this interference will make an increase of the anisotropy with detection frequency more pronounced, and will not change its sign. The difference with the results of ref 21 may be related to the system studied and the experimental parameters. In ref 21, the O−H stretch vibration of HDO was studied, which has a shorter vibrational lifetime T_1 than the O−D stretch vibration of HDO studied here. The shorter T_1 leads to a faster thermalization effect, which may affect the anisotropy already at early delays. Another difference with ref 21 is that we tune the excitation pulse further to the high-frequency wing of the absorption band, thus exciting a relatively large fraction of very weak (strained) hydrogen-bond configurations. As a result, in the present study the effect of the relaxation of these strained hydrogen-bond configurations on the anisotropy is more pronounced.

The frequency dependence of the anisotropy of the O−H stretch vibration of HDO has also been calculated with molecular dynamics simulations.[21,30] The calculated anisotropy shows a fast decay at early delay times that is largely due to librational motions. The calculated anisotropy does not show the decrease of the anisotropy with decreasing frequency that we observe in Figures 6A and 7A, following excitation in the far blue wing of the O−D stretch vibration. This difference may be due to the fact that the calculated short-time librational fluctuations have a relatively large amplitude that increases with frequency, thus leading to a rather strong decrease of the anisotropy with frequency. This strong frequency dependence of the librational contribution will make the effect of the relaxing strained hydrogen-bond configurations on the anisotropy less apparent in the simulations. The large amplitude of the calculated short-time librational fluctuations is probably due to the classical description of the librational motions.[21]

Spectral Diffusion. The decay of the first spectral moment also shows a slow component of which the time constant decreases from 0.7 ± 0.1 ps at 283 K to 0.3 ± 0.1 ps at 343 K. The presence of this spectral diffusion component agrees with the results of previous studies of the spectral diffusion of the O−D/O−H stretch vibrations of HDO in H_2O/D_2O. With different experimental techniques, it was found that the frequency−frequency correlation function of water possesses a slow component that decays on a time scale of ∼1 ps.[27,31−35] The slow component is also observed in molecular dynamics simulations[36−39] and can be assigned to changes in the hydrogen bond length due to the collective reorganization of the hydrogen-bond network of water.

The slow spectral diffusion process leads to a complete equilibration of the excited O−D oscillators over the absorption

band. As a result, the anisotropy will acquire the same value at all detection frequencies. It is indeed seen in Figures 6A and 7A that at all detection frequencies the anisotropy acquires the same value after ~1.5 ps. The time constant with which the anisotropy equilibrates is very similar to the time constant of the slow component of the spectral diffusion, as can be seen from the time constants shown in Figures 5B and 9.

Activation Energies of Spectral Relaxation and Reorientation. As is seen in Figure 5, the rapid spectral dynamics do not show a significant temperature dependence, which can be explained from the fact that these dynamics are associated with the relaxation of a strained, out-of-equilibrium configurational state. Hence, these dynamics do not involve any thermal activation. The time constant of the second, slow component of the spectral diffusion is observed to become shorter with increasing temperature, showing that the collective reorganization of the hydrogen-bond network becomes faster, in agreement with the results of refs 17 and 20. The speed up of the spectral equilibration also leads to a faster spectral equilibration of the anisotropy. The time constant of the decay of the slope of the anisotropy indeed shows a similar temperature dependence as the slow component of the spectral diffusion.

We determine the activation energies of the spectral relaxation and anisotropy relaxation by plotting the decay rates of the spectral diffusion, the anisotropy slope dynamics, and the equilibrated anisotropy in an Arrhenius plot (Figure 10). The spectral diffusion and the anisotropy dynamics show a

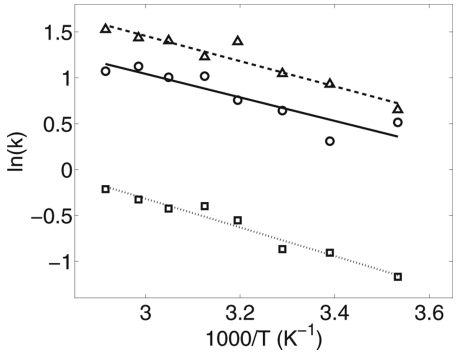

Figure 10. Natural logarithm of the decay rates of the slope of the anisotropy (triangles), the slow component of the decay of the first spectral moment (circles), and the long-time (average) anisotropy decay (squares) as a function of the inverse temperature. The activation energies are determined by fitting straight lines to the three sets of data points.

similar activation energy of 11 ± 2 kJ/mol (2.6 ± 0.5 kcal/mol). The activation energy of the averaged molecular reorientation is somewhat higher, showing a value of 14 ± 2 kJ/mol (3.3 ± 0.5 kcal/mol). This value agrees with previous studies that found activation energies of 16 ± 2 kJ/mol (3.6 ± 0.5 kcal/mol)[17,20] and 17 ± 2 kJ/mol (4.0 ± 0.5 kcal/mol).[18,19] The similar values of the activation energy of the reorientation and the spectral diffusion indicate that these processes are connected. This is not surprising, as water molecules need to evolve to the symmetrically strained (bifurcated) hydrogen-bond configuration before hydrogen-bond switching and thus reorientation can take place. The evolution to the transition state for reorientation is governed by the collective structural reorganization of the hydrogen-bond network, i.e., by the slow component of the spectral diffusion dynamics. Hence, a speed-up of the spectral diffusion dynamics implies a faster production of the transition state for reorientation, and thus an overall faster reorientation rate.

The activation energy of the molecular reorientation is somewhat higher than the activation energy of the spectral relaxation, and this difference may be significant. In ref 17, a similar difference was found: the activation energy of the spectral relaxation is 12 or 14 kJ/mol (depending on the method used), while the activation energy of the molecular reorientation is 16 kJ/mol. A comparison of the activation energies reported in previous studies points at a similar difference.[17−20] The higher activation energy of the molecular reorientation can be explained as follows. The effective rate of molecular reorientation is determined both by the rate of spectral diffusion and by the fraction of water molecules for which the hydrogen-bond configuration allows for hydrogen-bond switching (jump reorientation). A rise in temperature leads to a decrease of the average hydrogen-bond strength, and thus will increase the fraction of water molecules that can rapidly evolve to the transition states. The increase of the fraction of water molecules capable of hydrogen-bond switching implies an additional acceleration of the average molecular reorientation with temperature. Hence, the amount of acceleration with temperature and thus the activation energy is expected to be somewhat higher for the molecular reorientation than for the spectral diffusion.

CONCLUSIONS

We studied the mechanism of molecular reorientation of HDO molecules in H_2O with polarization-resolved two-color pump−probe experiments. We tuned the excitation pulse to the far blue wing of the O−D stretch vibration of the HDO molecules to selectively probe the spectral and reorientation dynamics of weakly hydrogen-bonded HDO molecules at temperatures between 283 and 342 K. In order to obtain an accurate determination of these dynamics, we corrected the transient spectra for the contributions of thermal effects. To this purpose, we performed a thorough study of the thermalization dynamics following vibrational relaxation by studying the thermal response in a separate experiment. The thermalization dynamics are particularly complex and important in the present study of weakly hydrogen-bonded O−D groups, because the excitation probability of the O−D vibrations is relatively low and because there is a significant probability of exciting the red wing of the absorption band of the O−H stretch vibrations of the H_2O solvent.

The first moment of the bleaching part of the transient spectrum shows a biexponential decay. The fast component of this decay with a time constant of ~100 fs is associated with the rapid relaxation of extremely strained hydrogen-bond configurations, i.e., configurations for which the length R_{O-O} of the hydrogen bond is long and/or for which the angle between the O−H coordinate and the O−O coordinate has a large value. Part of these strained hydrogen-bond configurations correspond to nearly symmetric bifurcated hydrogen-bond configurations in which the O−D group can switch its hydrogen-bonded partner. The excited strained hydrogen-bond configuration will rapidly relax to a configuration with a single strong hydrogen bond, and this relaxation is associated with a rapid red-shift of the O−D stretch vibrational frequency. The anisotropy of the transient spectral signals shows that the rapid relaxation also involves a strong change of the orientation of the excited O−D group. The time constant of this rapid

relaxation shows very little dependence on temperature which can be explained from the fact that the relaxation corresponds to a downhill relaxation of a strained out-of-equilibrium configuration. Hence, this relaxation is not thermally activated.

The slow component of the spectral relaxation with a time constant of ~0.7 ps at 293 K has been extensively studied before and is assigned to the collective structural reorganization of the hydrogen-bond network of liquid water. The time constant of this relaxation decreases by a factor of 2 going from 283 to 343 K, which corresponds to an activation energy of 11 ± 2 kJ/mol (2.6 ± 0.5 kcal/mol). The collective reorganization also leads to an equilibration of the anisotropy at different frequencies. For longer delays, the anisotropy shows the same exponential decay at all detection frequencies. This decay represents the average molecular reorientation of all water molecules. The time constant of the average molecular reorientation becomes shorter with increasing temperature, and its temperature dependence is similar to that of the collective structural reorganization. This similarity can be explained from the fact that water molecules need to evolve to the symmetrically strained (bifurcated) hydrogen-bond configuration before hydrogen-bond switching and thus reorientation can take place. Hence, acceleration of the collective hydrogen-bond reorganization speeds up the production of water molecules for which reorientation can take place and thus increases the rate of average molecular reorientation. The average molecular reorientation has an activation energy of 14 ± 2 kJ/mol (3.3 ± 0.5 kcal/mol), slightly higher than the activation energy of 11 ± 2 kJ/mol (2.6 ± 0.5 kcal/mol) of the collective structural reorganization of the hydrogen-bond network. The higher activation energy of the molecular reorientation suggests that a rise in temperature not only leads to an acceleration of the structural dynamics of the hydrogen-bonded network but also leads to an increase of the fraction of water molecules for which hydrogen-bond switching (jump reorientation) can occur.

■ ASSOCIATED CONTENT

Ⓢ Supporting Information

Description of the interference effects in frequency-dependent anisotropy along with a figure showing a simulation of the artifact that arises in the anisotropy in the case that the O−D stretch vibration in isotopically diluted water is excited by a narrow band pump centered in the blue wing of the absorption band. This material is available free of charge via the Internet at http://pubs.acs.org.

■ AUTHOR INFORMATION

Corresponding Author

*E-mail: bakker@amolf.nl.

Notes

The authors declare no competing financial interest.

■ ACKNOWLEDGMENTS

This work is part of the research program of the "Stichting voor Fundamenteel Onderzoek der Materie (FOM)", which is financially supported by the "Nederlandse organisatie voor Wetenschappelijk Onderzoek (NWO)".

■ REFERENCES

(1) Eisenberg, D.; Kauzmann, W. *The Structure and Properties of Water*; Oxford University Press: New York, 1969.

(2) Suresh, S.; Naik, V. Hydrogen Bond Thermodynamic Properties of Water from Dielectric Constant Data. *J. Chem. Phys.* **2000**, *113*, 9727−9732.

(3) Smith, D. W. G.; Powles, J. G. Proton spin-lattice Relaxation in Liquid Water and Liquid Ammonia. *Mol. Phys.* **1966**, *10*, 451−463.

(4) Godralla, B. C.; Zeidler, M. D. Molecular Dynamics in the System Water-dimethylsulfoxide. *Mol. Phys.* **1986**, *59*, 817−828.

(5) Hardy, E. H.; Zygar, A.; Zeidler, M. D.; Holz, M.; Sacher, F. D. Isotope Effect on the Translational and Rotational Motion in Liquid Water and Ammonia. *J. Chem. Phys.* **2001**, *114*, 3174−3181.

(6) Steinel, T.; Asbury, J. B.; Zheng, J.; Fayer, M. D. Watching Hydrogen Bonds Break: A Transient Absorption Study of Water. *J. Phys. Chem. A* **2004**, *108*, 10957−10964.

(7) Loparo, J. J.; Fecko, C. J.; Eaves, J. D.; Roberts, S. T.; Tokmakoff, A. Reorientational and Configurational Fluctuations in Water Observed on Molecular Length Scales. *Phys. Rev. B* **2004**, *70*, 180201-1−180201-4.

(8) Rezus, Y. L. A.; Bakker, H. J. On the Orientational Relaxation of HDO in Liquid Water. *J. Chem. Phys.* **2005**, *123*, 114502-1−114502-7.

(9) Woutersen, S.; Bakker, H. J. Resonant Intermolecular Transfer of Vibrational Energy in Liquid Water. *Nature* **1999**, *402*, 507−509.

(10) Cowan, M. L.; Bruner, B. D.; Huse, N.; Dwyer, J. R.; Chugh, B.; Nibbering, E. T. J.; Elsaesser, T.; Miller, R. J. D. Ultrafast Memory Loss and Energy Redistribution in the Hydrogen Bond Network of Liquid H_2O. *Nature* **2005**, *434*, 199−202.

(11) Piatkowski, L.; Eisenthal, K. B.; Bakker, H. J. Ultrafast Intermolecular Energy Transfer in Heavy Water. *Phys. Chem. Chem. Phys.* **2009**, *11*, 9033−9038.

(12) Yang, M.; Li, F.; Skinner, J. L. Vibrational Energy Transfer and Anisotropy Decay in Liquid Water: Is the Förster Model Valid? *J. Chem. Phys.* **2011**, *135*, 164505-1−164505-7.

(13) Ramasesha, K.; De Marco, L.; Mandal, A.; Tokmakoff, A. Water Vibrations have Strongly Mixed Intra- and Intermolecular Character. *Nat. Chem.* **2013**, *5*, 935−940.

(14) Laage, D.; Hynes, J. T. A Molecular Jump Mechanism of Water Reorientation. *Science* **2006**, *311*, 832−835.

(15) Lin, Y.-S.; Pieniazek, P. A.; Yang, M.; Skinner, J. L. On the Calculation of Rotational Anisotropy Decay, as Measured by Ultrafast Polarization-resolved Vibrational Pump-probe Experiments. *J. Chem. Phys.* **2010**, *132*, 174505-1−174505-11.

(16) Paesani, F.; Yoo, S.; Bakker, H. J.; Xantheas, S. S. Nuclear Quantum Effects in the Reorientation of Water. *J. Phys. Chem. Lett.* **2010**, *1*, 2316−2321.

(17) Nicodemus, R.; Corcelli, S.; Skinner, J.; Tokmakoff, A. Collective Hydrogen Bond Reorganization in Water Studied with Temperature-Dependent Ultrafast Infrared Spectroscopy. *J. Phys. Chem. B* **2011**, *115*, 5604−5616.

(18) Rønne, C.; Thrane, L.; Astrand, P. O.; Wallqvist, A.; Mikkelsen, K. V.; Keiding, S. R. Investigation of the Temperature Dependence of Dielectric Relaxation in Liquid Water by THz Reflection Spectroscopy and Molecular Dynamics Simulation. *J. Chem. Phys.* **1997**, *107*, 5319−5331.

(19) Petersen, C.; Tielrooij, K.-J.; Bakker, H. J. Strong Temperature Dependence of Water Reorientation in Hydrophobic Hydration Shells. *J. Chem. Phys.* **2009**, *130*, 214511-1−214511-6.

(20) Nicodemus, R.; Ramasesha, K.; Roberts, S.; Tokmakoff, A. Hydrogen Bond Rearrangements in Water Probed with Temperature-Dependent 2D IR. *J. Phys. Chem. Lett.* **2010**, *1*, 1068−1072.

(21) Ramasesha, K.; Roberts, S.; Nicodemus, A.; Mandal, R. A.; Tokmakoff, A. Ultrafast 2D IR Anisotropy of Water Reveals Reorientation during Hydrogen-bond Switching. *J. Chem. Phys.* **2011**, *135*, 054509-1−054509-11.

(22) Bakker, H. J.; Rezus, Y. L. A.; Timmer, R. L. A. Molecular Reorientation of Liquid Water Studied with Femtosecond Midinfrared Spectroscopy. *J. Phys. Chem. A* **2008**, *112*, 11523−11534.

(23) Rezus, Y. L. A.; Bakker, H. J. Strong Slowing Down of Water Reorientation in Mixtures of Water and Tetramethylurea. *J. Phys. Chem. A* **2008**, *112*, 2355−2361.

(24) Yang, M.; Skinner, J. L. Time-averaging Approximation in the Interaction Picture: Absorption Line Shapes for Coupled Chromophores with Application to Liquid Water. *J. Chem. Phys.* **2011**, *135*, 154114-1−154114-6.
(25) Lock, A. J.; Bakker, H. J. Temperature Dependence of Vibrational Relaxation in Liquid H2O. *J. Chem. Phys.* **2002**, *117*, 1708−1713.
(26) Tielrooij, K. J.; Petersen, C.; Rezus, Y. L. A.; Bakker, H. J. Reorientation of HDO in Liquid H2O at Different Temperatures: Comparison of First and Second Order Correlation Functions. *Chem. Phys. Lett.* **2009**, *471*, 71−74.
(27) Loparo, J. J.; Roberts, S. T.; Tokmakoff, A. Multidimensional Infrared Spectroscopy of Water. II. Hydrogen Bond Switching Dynamics. *J. Chem. Phys.* **2006**, *125*, 194522-1−194522-12.
(28) Fecko, C. J.; Loparo, J. J.; Roberts, S. T.; Tokmakoff, A. Local Hydrogen Bonding Dynamics and Collective Reorganization in Water: Ultrafast Infrared Spectroscopy of HOD/D2O. *J. Chem. Phys.* **2005**, *122*, 054506-1−054506-18.
(29) Moilanen, D. E.; Fenn, E. E.; Lin, Y.; Skinner, J. L.; Bagchi, B.; Fayer, M. D. Water Inertial Reorientation: Hydrogen Bond Strength and the Angular Potential. *Proc. Natl. Acad. Sci. U.S.A.* **2008**, *105*, 5295−5300.
(30) Stirnemann, G.; Hynes, J.; Laage, D. Water Hydrogen Bond Dynamics in Aqueous Solutions of Amphiphiles. *J. Phys. Chem. B* **2010**, *114*, 3052−3059.
(31) Gale, G. M.; Gallot, G.; Hache, F.; Lascoux, N.; Bratos, S.; Leicknam, J.-C. Femtosecond Dynamics of Hydrogen Bonds in Liquid Water: A Real Time Study. *Phys. Rev. Lett.* **1999**, *82*, 1068−1071.
(32) Woutersen, S.; Bakker, H. J. Hydrogen Bond in Liquid Water as a Brownian Oscillator. *Phys. Rev. Lett.* **1999**, *83*, 2077−2080.
(33) Stenger, J.; Madsen, D.; Hamm, P.; Nibbering, E. T. J.; Elsaesser, T. A Photon Echo Peak Shift Study of Liquid Water. *J. Phys. Chem. A* **2002**, *106*, 2341−2350.
(34) Yeremenko, S.; Pshenichnikov, M. S.; Wiersma, D. A. Hydrogen-bond Dynamics in Water Explored by Heterodyne-detected Photon Echo. *Chem. Phys. Lett.* **2003**, *369*, 107−113.
(35) Asbury, J. B.; Steinel, T.; Stromberg, C.; Corcelli, S. A.; Lawrence, C. P.; Skinner, J. L.; Fayer, M. D. Water Dynamics: Vibrational Echo Correlation Spectroscopy and Comparison to Molecular Dynamics Simulations. *J. Phys. Chem. A* **2004**, *108*, 1107−1119.
(36) Rey, R.; M?ller, K. B.; Hynes, J. T. Hydrogen Bond Dynamics in Water and Ultrafast Infrared Spectroscopy. *J. Phys. Chem. A* **2002**, *106*, 11993−11996.
(37) Lawrence, C. P.; Skinner, J. L. Vibrational Spectroscopy of HOD in Liquid D2O. III. Spectral Diffusion, and Hydrogen-Bonding and Rotational Dynamics. *J. Chem. Phys.* **2003**, *118*, 264−272.
(38) Corcelli, S. A.; Lawrence, C. P.; Skinner, J. L. Combined Electronic Structure/molecular Dynamics Approach for Ultrafast Infrared Spectroscopy of Dilute HOD in Liquid H2O and D2O. *J. Chem. Phys.* **2004**, *120*, 8107−8117.
(39) Auer, B.; Kumar, R.; Schmidt, J. R.; Skinner, J. L. Hydrogen Bonding and Raman, IR, and 2D-IR Spectroscopy of Dilute HOD in Liquid D2O. *Proc. Natl. Acad. Sci. U.S.A.* **2007**, *104*, 14215−14220.

Supplementary Information to: Femtosecond mid-infrared study of the reorientation of weakly hydrogen-bonded water molecules

Sietse T. van der Post and Huib J. Bakker*

FOM Institute AMOLF, Science Park 104, Amsterdam, The Netherlands

(Dated: February 3, 2014)

*Electronic address: bakker@amolf.nl

I. INTERFERENCE EFFECTS IN THE FREQUENCY-DEPENDENT ANISOTROPY

In this section we will describe in detail the amplification effect of a frequency dependence in the anisotropy signals of an excited anharmonic vibration. We assume a similar excitation spectrum as was used in the experiment, with a FWHM of 60 cm^{-1} and centered at 2650 cm^{-1}. The isotropic transient spectra are written as the product of the population dynamics $N(t)$, reflecting the vibrational decay of the excitation, and the excited state transient absorption spectrum $\sigma(\nu)$. Furthermore, $\sigma(\nu)$ consists of a negative contribution $\sigma_{01}(\nu)$ due to stimulated emission and ground state depletion (the bleach) at the $\nu_s = 0 \rightarrow 1$ transition frequency and a positive contribution $\sigma_{12}(\nu)$ due to excited state absorption at the $\nu_s = 1 \rightarrow 2$ transition frequency. The heat corrected isotropic transient spectra $\Delta\alpha_{\mathrm{iso}}(\nu, t)$ for a single species solution can thus be written as,

$$\Delta\alpha_{\mathrm{iso}}(\nu, t) = N(t)\sigma(\nu) = N(t)\left(\sigma_{01}(\nu) + \sigma_{12}(\nu)\right) \tag{1}$$

However, the absorption spectrum of O–D oscillators in isotopically diluted water is inhomogeneously broadened: oscillators with stronger or weaker hydrogen-bonds have their resonance frequency at different positions in the absorption band. A narrow band excitation pulse with its center frequency in the blue wing of the O–D stretch absorption band will result in a blue-shifted transient response of both $\sigma_{01}(\nu)$ and $\sigma_{12}(\nu)$ at time zero. Due to spectral diffusion, σ_{01} and σ_{12} have a time dependence and will eventually assume their equilibrium shape.

For simplicity we consider a gaussian shape for the bleach with central frequency ν_c^0 at time zero, exponentially relaxing to ν_c^∞ due to spectral diffusion with rate k_s. The spectral contribution of the bleach $\sigma_{01}(\nu, t)$ to the total transient absorption can then be written as,

$$\sigma_{01}(\nu, t) = Ae^{-\frac{(\nu-\nu_c(t))^2}{2\Sigma^2}} \tag{2}$$

where A is the amplitude of the response and Σ the width of the gauss. We ignored here the fact that a narrow-band excitation also leads to a time-dependent broadening of Σ. The time-dependent center frequency $\nu_c(t)$ can be written as,

$$\nu_c(t) = (\nu_c^0 - \nu_c^\infty)e^{-k_s t} + \nu_c^\infty \tag{3}$$

A similar relation can be derived for the spectral contribution of the induced absorption $\sigma_{12}(\nu, t)$, for which the sign of the amplitude will be different and the center frequency is shifted to the red side of the spectrum by the anharmonicity (180 cm^{-1}). Using the expression for the anisotropy

yields,

$$R_m(\nu,t) = \frac{\sigma_{01}(\nu,t)R_{01}(\nu,t) + \sigma_{12}(\nu,t)R_{12}(\nu,t)}{\sigma_{01}(\nu,t) + \sigma_{12}(\nu,t)} \tag{4}$$

The subscript m of the anisotropy R_m is added as a reminder that this parameter represents the measured anisotropy as opposed to the actual anisotropy of the bleaching R_{01} and the induced absorption R_{12}. We explicitly took the anisotropy different for the bleach and the induced absorption. This is necessary because at a given frequency ν the spectral response of the bleach arises from different oscillators than the spectral response of the induced absorption, due to the anharmonicity of the OD stretch vibration. An oscillator that contributes to the bleach at 2500 cm^{-1}, therefore also contributes to the induced absorption at 2320 cm^{-1}. In terms of the associated anisotropy dynamics we write this as:

$$R_{12}(\nu,t) = R_{01}(\nu + 180, t) \tag{5}$$

In case there is no frequency dependence in the anisotropy, the equality in Eq. (5) is trivial and $R_m(\nu,t)$ reduces to $R_{01}(t)$. For the experiment in this work, the anisotropy in fact does depend on the probe frequency. In line to what we found we define the frequency dependence as,

$$R_{01}(\nu,t) = \frac{2}{5}\left(0.25e^{-0.4t} + 0.15\rho e^{-3t}\right) \begin{cases} \rho = 0\,(\nu < 2500) \\ \rho = \frac{\nu - 2500}{100}\,(2500 < \nu < 2600) \\ \rho = 1\,(\nu > 2600) \end{cases} \tag{6}$$

We calculated $R_m(\nu,t)$ according to Eq. (4) for values of the spectral diffusion parameters that are describing the measured data as presented in the main text of this manuscript. The results are plotted in Fig. 1 for a number of probe-frequencies. The black lines represent the actual anisotropy dynamics of the bleach at 2500 cm^{-1} and 2650 cm^{-1} (Eq. (6)). As can be seen, the amplitude of R_m is heavily suppressed for short delay times, especially at frequencies close to 2500 cm^{-1}. R_m even shows an asymptotic behavior. This asymptotic behavior follows from the denominator of Eq. (4) than can become very small for frequencies at which $\sigma_{01}(\nu,t) \sim \sigma_{12}(\nu,t)$. Due to the difference between $R_{01}(\nu,t)$ and $R_{12}(\nu,t)$, the numerator is not necessarily small at these frequencies. This effect disappears for longer delay times for two reasons. 1) The frequency dependence of $R_{01}(\nu,t)$ and $R_{12}(\nu,t)$ decreases with increasing t, and 2) the zero-crossing of $\sigma(\nu,t)$ shifts to frequencies lower than 2500 cm^{-1}, thereby diminishing the artefact. Both of these points are due to spectral diffusion. In case spectral diffusion would not be complete within the timescale of the experiment, $R_{01}(\nu,t)$ and $R_{12}(\nu,t)$ would not lose their frequency dependence

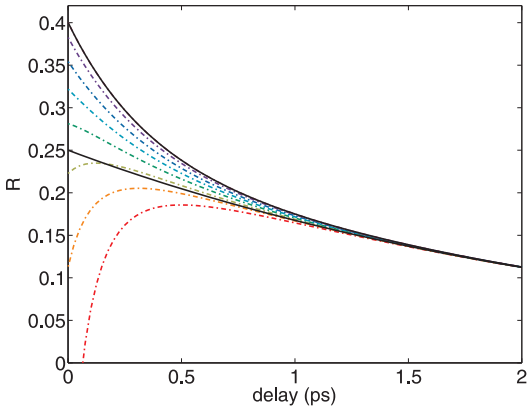

FIG. 1: A simulation of the artefact that arises in the anisotropy in case the O–D stretch vibration in isotopically diluted water is excited by a narrow band pump centered in the blue wing of the absorption band. The solid black lines are the actual anisotropy dynamics at 2500 cm^{-1} (lower line) and 2600 cm^{-1} (upper line). The dashed-dotted lines are the anisotropy dynamics that were calculated as they would be measured for equidistant frequencies between 2500 cm^{-1} (lowest curve) and 2600 cm^{-1} (highest curve) (step size 12.5 cm^{-1}).

and the measured anisotropy $R_m(\nu, t)$ would retain a frequency dependence.